



Contents lists available at ScienceDirect

Journal of Colloid and Interface Science

www.elsevier.com/locate/jcis



A synthetically modified hydrophobin showing enhanced fluororous affinity



Roberto Milani^{a,c,*}, Lisa Pirrie^{b,d}, Lara Gazzera^d, Arja Paananen^b, Michele Baldrighi^d,
Evanthia Monogioudi^b, Gabriella Cavallo^d, Markus Linder^{b,e,*}, Giuseppe Resnati^{c,d,*},
Pierangelo Metrangolo^{b,c,d,*}

^aVTT Technical Research Centre of Finland Ltd, Biologinkuja 7, Espoo FI-02044 VTT, Finland

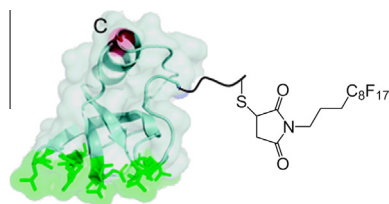
^bVTT Technical Research Centre of Finland Ltd, Tietotie 2, Espoo FI-02044 VTT, Finland

^cCenter for Nano Science and Technology@Polimi, Istituto Italiano di Tecnologia, Via G. Pascoli 70, I-20133 Milano, Italy

^dNFMLab-DCMIC “Giulio Natta”, Politecnico di Milano, Via L. Mancinelli 7, I-20131 Milano, Italy

^eAalto University, School of Chemical Technology, Kemistintie 1, P.O. Box 16100, FI-00076 AALTO Espoo, Finland

GRAPHICAL ABSTRACT



ARTICLE INFO

Article history:

Received 27 November 2014

Accepted 2 February 2015

Available online 9 February 2015

Keywords:

Hydrophobin
Surfactant protein
Protein film formation
Fluorinated material
Fluororous tag
Compatibilization

ABSTRACT

Hydrophobins are natural surfactant proteins endowed with exceptional surface activity and film-forming capabilities and their use as effective “fluorine-free fluorosurfactants” has been recently reported. In order to increase their fluorophilicity further, here we report the preparation of a unique fluororous-modified hydrophobin, named F-HFBI. F-HFBI was found to be more effective than its wild-type parent protein HFBI at reducing interface tension of water at both air/water and oil/water interfaces, being particularly effective at the fluororous/water interface. F-HFBI was also found to largely retain the exceptionally good capability of forming strong and elastic films, typical of the hydrophobin family. Further studies by interface shear rheology and isothermal compression, alongside Quartz Crystal Microbalance and Atomic Force Microscopy, demonstrated the tendency of F-HFBI to form thicker films compared to the wild-type protein. These results suggest that F-HFBI may function as an effective compatibilizer for biphasic systems comprising a fluororous phase.

© 2015 The Authors. Published by Elsevier Inc. This is an open access article under the CC BY-NC-ND license (<http://creativecommons.org/licenses/by-nc-nd/4.0/>).

* Corresponding authors at: VTT Technical Research Centre of Finland Ltd, Biologinkuja 7, Espoo, FI-02044 VTT, Finland (R. Milani), VTT Technical Research Centre of Finland Ltd, Tietotie 2, Espoo, FI-02044 VTT, Finland (M. Linder and P. Metrangolo), NFMLab-DCMIC “Giulio Natta”, Politecnico di Milano, Via L. Mancinelli 7, I-20131 Milano, Italy (G. Resnati). Fax: +39 0223993180 (G. Resnati and P. Metrangolo).

E-mail addresses: roberto.milani@vtt.fi (R. Milani), ext-lisa.pirrie@vtt.fi (L. Pirrie), lara.gazzera@polimi.it (L. Gazzera), arja.paananen@vtt.fi (A. Paananen), michele.baldrighi@iit.it (M. Baldrighi), evanthia.monogioudi@ec.europa.eu (E. Monogioudi), gabriella.cavallo@polimi.it (G. Cavallo), markus.linder@aalto.fi (M. Linder), giuseppe.resnati@polimi.it (G. Resnati), pierangelo.metrangolo@polimi.it (P. Metrangolo).

1. Introduction

Hydrophobins (HFBS) are small (<100 amino acids) proteins produced by filamentous fungi that are endowed with surface activity and film-forming capabilities unmatched by any other protein [1]. HFBS are exceptionally stable towards denaturation due to the presence of four disulfide bridges in their core structure, and are able to withstand temperatures close to the boiling point of water [2–4]. The high surface activity of HFBS is due to their

<http://dx.doi.org/10.1016/j.jcis.2015.02.003>

0021-9797/© 2015 The Authors. Published by Elsevier Inc.

This is an open access article under the CC BY-NC-ND license (<http://creativecommons.org/licenses/by-nc-nd/4.0/>).

Janus-type structure where a discrete and well-defined portion of the protein surface is comprised of hydrophobic amino acids and known as the hydrophobic patch, while the remaining surface is hydrophilic in nature [5,6]. The most distinguishing feature of the HFBs is their ability to self-assemble into strong and elastic films at the interface between hydrophilic and hydrophobic phases. Such films have also been reported to be orders of magnitude stronger than those formed by other surface active proteins including β -lactoglobulin and β -casein [7]. Recently, we have demonstrated that HFBs also function as particularly effective “fluorine-free fluorosurfactants” reducing interface energy at the fluorous [8–10]/aqueous interface [11].

The remarkable performance differences between fluorocarbon (FC) and hydrocarbon (HC) surfactants originate from the peculiar features of the fluorine atom such as low polarizability, high electronegativity and ionization potential, as well as a larger size compared to the hydrogen atom. FC chains are thus more hydrophobic than their HC counterparts, and are also substantially lipophobic [12]. One first consequence is that FC-surfactants are more effective in lowering the surface tension of water, being able to attain values as low as 15–20 mN/m, whereas typical HC-based amphiphiles can only reach values of about 30–40 mN/m [13–15]. A second consequence is that FCs tend to segregate into a separate phase in order to avoid unfavorable interactions with other molecules, either hydrophilic or lipophilic, a phenomenon known as *fluorophobic effect* [8–10,16–18].

With the objective of further improving the performance of HFBs at fluorous/aqueous interfaces, and to combine their exceptional film forming capabilities with the superior surface activity of FC-surfactants, we covalently bound a FC chain to the exposed surface of the protein NCysHFBI, which is a genetically engineered variant of the wild-type (WT) hydrophobin HFBI. In this way we obtained a unique fluorous-modified hydrophobin, termed F-HFBI [19].

Protein fluorination strategies have to date mainly relied on the introduction of selectively fluorinated amino acids, typically leucines, in the protein primary structure [20–27]. An alternative approach consists of the site-specific derivatization with fluorous tags by covalently binding FC residues to peptides and proteins, mainly for immobilization, separation, and enrichment purposes [28–31]. Expanding on this strategy, here we report the preparation and subsequent characterization of a HFB derivative covalently functionalized with a single perfluorooctyl chain. This specific FC segment was selected based on the ready availability of reagents, and is intended to act as a first model for the introduction of more environmentally compliant moieties, e.g., small perfluoropolyether chains.

2. Materials and methods

2.1. Materials

NCysHFBI was produced using recombinant strains of *T. reesei*, purified by RP-HPLC as described previously and lyophilized before use. [32] Galden® SV90 (GSV90) is a low molecular weight perfluoropolyether fluid (90 °C boiling point) produced by Solvay Specialty Polymers. Heptane, hexadecane, 1H,1H,2H,2H-perfluorodecane-1-thiol, 11-mercapto-1-undecanol, and hexanethiol were purchased from Sigma Aldrich and used without further purification.

2.2. Reduction of NCysHFBI

The starting protein NCysHFBI was first reduced in order to break the dimers occurring on the formation of disulfide bridges involving the accessible Cys residues close to the N terminus of the protein. Typically, 10 mg of NCysHFBI were dissolved in

1.6 mL of mQ water, then 80 μ L of acetate buffer (1 M, pH 5), 32.5 μ L of 0.5 M EDTA and 1660 μ L of 0.1 M dithiothreitol were sequentially added. The mixture was incubated for 1 h at 37 °C, and the reduced NCysHFBI was purified by reverse phase HPLC on a Vydac C4 column using a gradient of water/acetonitrile (both containing 0.1% TFA). Following overnight freeze-drying, the typical yield of the reaction was around 50–60%. The reduced protein was stored at –80 °C. MALDI-TOF: m/z = 8677.

2.3. Preparation of F-HFBI

In a typical synthesis, 5 mg of reduced NCysHFBI were dissolved in a mixture of 2 mL THF and 3.5 mL phosphate buffer (0.1 M, pH 7.2). A solution of 5.8 mg of 3-(perfluorooctyl)-propyl-1-maleimide in 1.5 mL THF was added. The vial containing the mixture was briefly flushed with nitrogen, wrapped in aluminium foil, and gently stirred at room temperature for 5 h. The solution was lyophilized overnight, then the solid was redissolved in 2.5 mL of 50% EtOH for purification by reverse phase HPLC on a Vydac C4 column using a gradient of water/acetonitrile (both containing 0.1% TFA). F-HFBI was subsequently freeze-dried and recovered typically in 65–70% yield. MALDI-TOF: m/z = 9232.

2.4. Zeta-potential measurements

The isoelectric point of F-HFBI was measured experimentally with a Nano-ZS zetasizer (Malvern instruments, UK) by performing titrations with 0.01 M and 0.1 M NaOH on 0.10 mg/mL F-HFBI solutions in mQ water. The measurements were highly reproducible, and the experimental pI obtained as an average of two different measurements was 4.87 (Fig. S1 in the Supporting information).

2.5. MALDI-TOF Spectrometry

An Autoflex II instrument from Bruker Daltonics (Bremen, Germany) equipped with a UV/N₂-laser (337 nm/100 μ J) was used to carry out mass spectrometric analyses. Saturated α -cyano-4-hydroxycinnamic acid in a 1:2 (v/v) mixture of acetonitrile and aqueous 0.1% (v/v) trifluoroacetic acid was used as a matrix. The purified NCysHFBI and F-HFBI were dissolved in the same solvent mixture at about 2 mg/mL concentration, mixed with the matrix solutions in 1:1 (v/v) ratio and applied on the stainless steel target plate in 1 μ L aliquots. The sample spot was dried in air at room temperature. The mass spectrum (4–20 kDa) was measured in linear positive-ion mode, and Protein standard solution I (Bruker Daltonics) was used for the external molecular mass calibration.

2.6. CD spectroscopy

CD spectra were collected with a Chirascan spectrophotometer (Applied Photophysics) fitted with a Peltier temperature controller, using a rectangular quartz cuvette with an optical path length of 1 mm. Data acquisition was performed in steps of 0.5 nm at a wavelength range from 190 to 280 nm with a spectral bandwidth of 1.0 nm. All spectra were corrected in baseline with mQ water as the blank. Spectra were the average of 10 consecutive scans. The signals were normalized to mean residue ellipticity (MREs) based on the peptide concentration:

$$[\theta]_{\lambda} = \frac{\theta_{obs}}{(10 \times l \times c \times (n-1))}$$

where $[\theta]_{\lambda}$ is the MRE at wavelength λ in deg cm² dmol⁻¹, l is the path length in cm, c is the molar concentration and $(n-1)$ is the number of peptide bonds.

2.7. Solubility assessment

For solubility determination at room temperature (25 °C), a saturated aqueous solution of either HFBI or F-HFBI was prepared and the suspension was placed in an ultrasound bath for 30 min. Following thermo-mixing (25 °C, 1000 rpm) for 1 h, the suspension was filtered through a 0.22 µm PTFE membrane filter into a pre-weighed Eppendorf vial. The water was removed by Speedvac and the amount of protein in the vial weighed. Measured solubilities in water were 3.0 mg/mL for HFBI and 1.9 mg/mL for F-HFBI. The method was repeated at higher temperatures where sonication was achieved at 40 °C and thermo-mixing at 80 °C, yielding water solubility values of 16.8 mg/mL for HFBI and 11.0 mg/mL for F-HFBI. Both proteins were essentially insoluble in either heptane or GSV90 regardless of the temperature.

2.8. Interfacial tension measurements

Interface tensiometric measurements were performed on a CAM 200 (KSV Instruments Ltd) and the built-in software CAM 2008 was used for data processing. A 15 µL droplet of Golden SV90 was injected into 900 µL of a freshly prepared solution of HFBI or F-HFBI solution in mQ water (10 µM concentration) contained in a quartz cuvette. For measurements at the interface with air and hexadecane, a 15 µL droplet of 10 µM HFBI or F-HFBI aqueous solution was left hanging in air or in hexadecane within a quartz cuvette from the syringe needle. The interfacial energies were derived from the fitting of the droplet shape by the Young–Laplace method.

2.9. Interfacial shear rheology

All measurements were performed on an AR-G2 stress controlled rheometer (TA Instruments) equipped with a Pt-Ir du Noüy ring (13 mm diameter) which was flamed prior to use. Before experiments were commenced the inertia of the instrument was calibrated and the response mapped in order to confirm the linear response of the instrument. All measurements were carried out at room temperature (25 °C) and the system was allowed to equilibrate for 1 min prior to each measurement. GSV90 (33 g) was poured into a round glass vessel (65 mm diameter) and the du Noüy ring was positioned 0.5 cm above the surface. A freshly prepared solution of protein (HFBI or F-HFBI, 100 µL, 1 mg/mL) was spread on the surface using a 10 µL glass syringe followed by 30 mL of mQ water. The ring was then raised to the interface and the experiments started approximately 5 min after spreading the protein solution. A time sweep over 10 h was first performed (strain 0.05%, frequency 0.1 Hz) followed by a frequency sweep (strain 0.05%, frequency range 0.01–10 Hz), a strain sweep (strain 10⁻³–1%, frequency 0.1 Hz) and an additional time sweep over 16 h. The frequency and strain sweep data are reported in Fig. S2.

2.10. Isothermal compression by Langmuir trough

Isothermal compression measurements were performed on a KSV Minimicro trough using a Pt Wilhelmy plate at a constant temperature of 21 °C. F-HFBI was first dissolved at 21.6 µM concentration in a mixture of 20% (v/v) acetonitrile in 20 mM phosphate buffer (pH 7.2). 350 µL of the freshly prepared protein solution were spread onto a 20 mM phosphate buffer (pH 7.2) subphase, and the system was allowed to rest for 1 h before starting the measurement, which was performed at a compression rate of 300 mm²/min.

2.11. QCM-D

All experiments were carried out on a Q-Sense E4 instrument (Q-Sense). Au sensors (Q-Sense, Biolin Scientific) were cleaned prior to use in a UV/ozone chamber for 10 min followed by immersion in a mixture of H₂O:NH₃:H₂O₂ (5:1:1) at 75 °C for 10 min. The sensors were rinsed thoroughly with mQ water and dried with nitrogen before being subjected to further UV/ozone treatment for 10 min. Functionalization was achieved by immersion of the chips in 0.05 M ethanolic solutions of 1H,1H,2H,2H-perfluorodecane-1-thiol, 11-mercapto-1-undecanol or hexanethiol. Following rinsing with ethanol and mQ water, the Au sensors were dried with nitrogen and mounted into the measurement chamber of the QCM-D (pre-calibrated to 23 °C). Proteins were dissolved in 50 mM PBS containing 20% acetonitrile (0.1 mg/mL for HFBI; 0.1226 mg/mL for F-HFBI) and 500 µL of protein solution were pumped through the measurement chamber at a flow rate of 0.1 mg/mL. The sensors were allowed to equilibrate in zero-flow condition for 30 min before being rinsed with the running buffer in order to remove excess protein. For HFBI, where the dissipation values were close to zero and the frequencies of the various overtones were the same, thus indicating an essentially elastic film, the Sauerbrey relationship was used to estimate the mass of adsorbed protein [33]. For this calculation, the third overtone was used. For F-HFBI, where the dissipation values were larger than zero, the adsorbed mass of protein was estimated using the QTools software, applying the Voigt viscoelastic model [34] to overtones 3, 5, 7, 9 and 11. This model consists of a spring and a dashpot in parallel and is particularly suitable for more rigid rather than liquid-like viscoelastic soft matter materials.

2.12. AFM

Topography images of HFBI and F-HFBI films adsorbed on QCM crystals were captured with an atomic force microscope. A Nano ScopeV Multimode8 AFM (E scanner, Bruker) and ScanAsyst-Air cantilevers (Bruker, $f_0 = 50\text{--}90$ kHz, $k = 0.4$ N/m) were used in all measurements. All images were recorded in the ScanAsyst mode in air with scan rate 1 Hz. Images were only flattened to remove possible tilt in the image data, and no further processing was done. The NanoScope Analysis software (Bruker) was used for image processing and analysis.

3. Results and discussion

3.1. Preparation and characterization of F-HFBI

The functionalization was performed by standard thiol-maleimide coupling chemistry on NCysHFBI, an engineered variant of the WT-HFBI expressed from *Trichoderma Reesei* (Fig. 1a) [35]. The NCysHFBI variant contains an N-terminal extension of 13 amino acids where one residue is an accessible cysteine capable of selective reaction with maleimide derivatives. MALDI-TOF mass spectrometry confirmed the identity of the product (Fig. S3 in the Supporting information), which has a molecular weight of 9.23 kDa and a degree of purity $\geq 90\%$ as estimated from analytical HPLC (Fig. 1b; the full chromatograms are reported in Fig. S4 in the Supporting information). While some unreacted NCysHFBI can be seen in the MALDI spectrum, its amount appears to be very small in the analytical HPLC chromatogram of purified F-HFBI. The only other small peaks observed by MALDI follow a pattern which was observed also for NCysHFBI and are attributable to protein glycosylation. Therefore, the $\leq 10\%$ impurity appearing as a shoulder peak in the analytical HPLC chromatogram of F-HFBI may be due to non-site-selective fluorination occurring to a small extent, likely by reaction with amino moieties. Fluorination of any of the eight

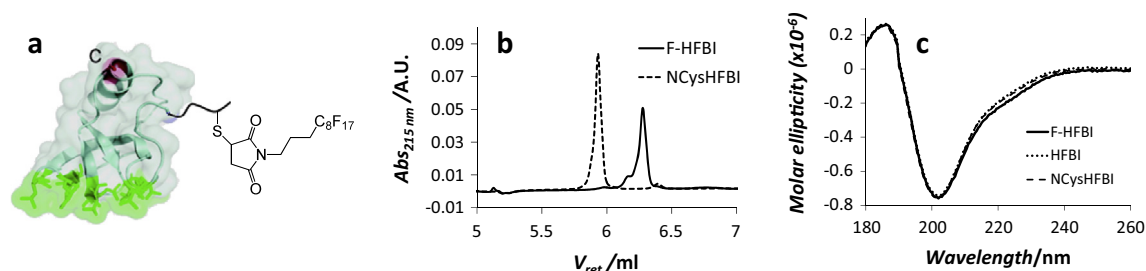


Fig. 1. (a) Schematic representation of the synthesized F-HFBI; (b) Analytical HPLC chromatogram of purified F-HFBI, compared with reduced NCysHFBI (a blank run performed with only mQ water as sample was used for baseline subtraction); (c) Normalized CD spectra of HFBI, NCysHFBI, and F-HFBI.

cysteines internal to the protein is to be excluded, due to the inaccessibility of these residues which are engaged in four disulfide bridges considered essential for hydrophobin folding. This is also consistent with the fact that the secondary structural elements for F-HFBI were almost identical to both the parent proteins NCysHFBI and the WT-HFBI (Fig. 1c), confirming that the modification did not significantly affect the folding of F-HFBI. A small change can be observed around 225 nm in the F-HFBI spectrum, which is indicative of a slight increase in the α -helix content, as previously observed for HFBI assembled on the surface of Teflon[®] nanoparticles [3].

Solubility studies revealed that F-HFBI is less soluble in water than WT-HFBI (2 mg/mL versus 3 mg/mL at 25 °C), consistent with the addition of the highly hydrophobic FC chain. Both proteins were essentially insoluble in both highly fluorinated (Galden SV90, here abbreviated as GSV90) and lipophilic (hexadecane) solvents even at 80 °C.

3.2. Surface activity and film formation

The ability of F-HFBI to reduce interfacial tension was probed for 10 μ M protein aqueous solutions at the interface with a fluororous phase (GSV90), a lipophilic phase (hexadecane), and air. The

results were compared to those obtained with equimolar solutions of the WT-HFBI (Fig. 2a–c).

The fluorinated protein F-HFBI was found to be more effective than the WT one at reducing the interfacial tension between water and the hydrophobic liquid phases, and its stabilizing effect was especially evident at the fluororous/aqueous interface, where the difference in the interface energy reduction promoted by the two proteins is higher than 10 mN/m. The observed trend of interface tension versus time is typical for HFBI where a rapid initial decrease in surface tension, attributed to protein absorption at the interface, is followed by a subsequent slower reduction, which is associated with a re-arrangement of the protein film. The two proteins behave similarly at the aqueous/air interface where F-HFBI appeared to follow slightly slower kinetics during the initial self-assembly process, although reaching lower values. These results confirm that the presence of the FC chain effectively enhanced the surface activity of the protein, particularly at the fluororous/aqueous interface, as expected.

F-HFBI was also found to maintain the typical film-forming capability of the HFBI family as confirmed by the formation in twenty minutes of a visible thin film around a droplet of an aqueous protein solution in air. As a result of water evaporation, causing a decrease in the surface area of the droplet, the assembled protein film contracted to afford the characteristic wrinkles typical of HFBI

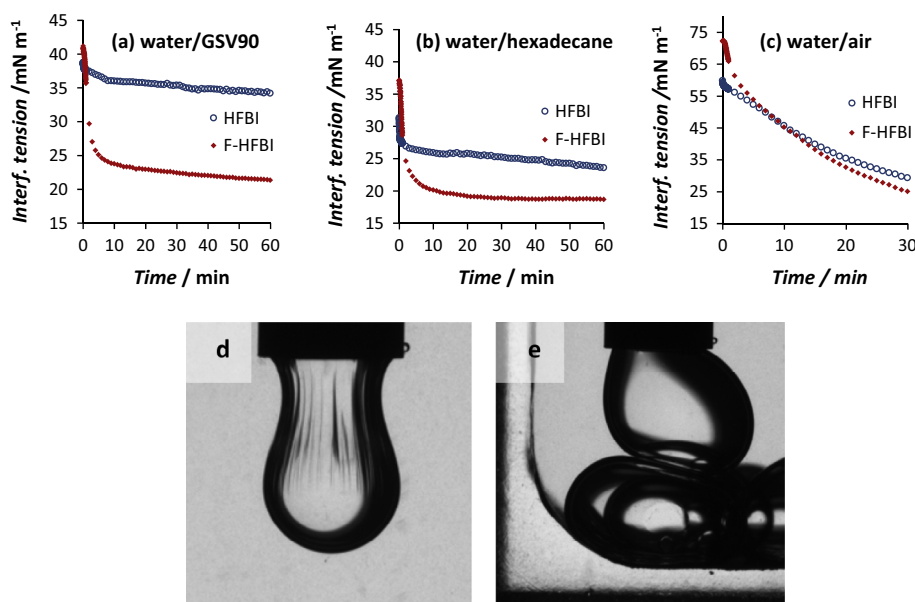


Fig. 2. Top: Plots of interface tension versus time at the interface between 10 μ M aqueous protein solution and (a) GSV90, (b) hexadecane, and (c) air. Bottom: (d) Protein film formed at the interface between a droplet of GSV90 and an aqueous F-HFBI solution; (e) GSV90 droplets generated inside an aqueous F-HFBI solution do not coalesce even when moderate pressure is applied (see video in the Supporting information).

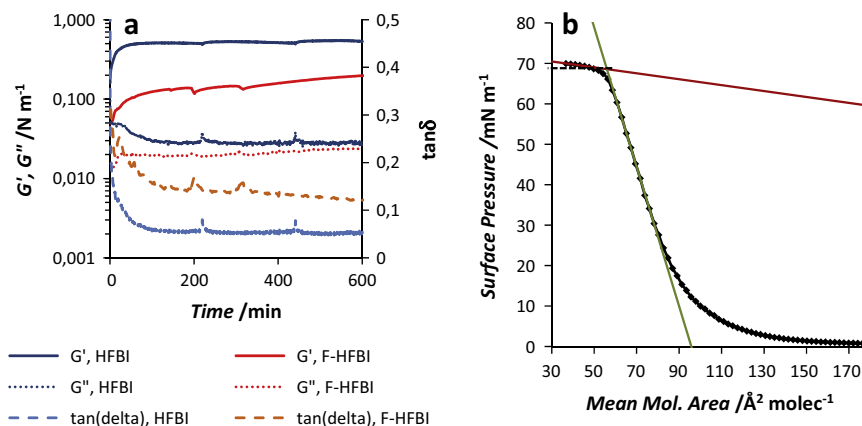


Fig. 3. (a) Interface shear rheology for HFBI and F-HFBI films at the GSV90/water interface (time sweep). (b) Isothermal compression of a F-HFBI film in a Langmuir trough.

films. The same phenomenon was also observed at liquid–liquid interfaces, for example between a perfluoropolyether fluid droplet (GSV90) and a surrounding aqueous F-HFBI solution. By simply drawing back a small portion of the droplet liquid into the syringe, the protein film became visible (Fig. 2d). At F-HFBI concentrations of 10 μM , a protein film was formed within seconds of droplet generation. The film is sufficiently strong to prevent the coalescence of fluoros droplets into a single phase, even when moderate pressure is applied (Fig. 2e; a short movie illustrating the experiment is available in the Supporting information).

3.3. Rheological and structural studies of the protein film

In order to gather quantitative information on the strength of the F-HFBI formed film, investigations by interfacial shear rheology were carried out. The F-HFBI film was formed at the interface between GSV90 and water and its elastic and loss moduli were measured and compared to those of a WT-HFBI film prepared under analogous conditions (Fig. 3a and Fig. S2 in the Supporting information).

Both films appeared to be elastic in nature and their G' values were significantly higher than those previously reported for other surface active proteins or phospholipids at water/air and water/oil interfaces [36–40] thus demonstrating the exceptional properties of these proteins. However, rheology showed some clear differences between the WT-HFBI and F-HFBI. The increase over time in the elastic modulus of the F-HFBI film was observed to be slower than the one of the WT-protein. In particular, while a plateau was reached within one hour with the WT-HFBI, the elastic modulus of the F-HFBI film was still slowly rising after ten hours. Moreover, the F-HFBI film displayed lower G' values and higher loss factor $\tan(\delta)$ values than the WT film. These observations indicate that the film formed by F-HFBI, whilst still being exceptionally strong and elastic for a protein film, is slightly weaker and more viscous in nature than the film formed by the WT-HFBI. Furthermore, the continued build-up over a longer time of F-HFBI films may be the result not only of slower self-assembly but also of a propensity of F-HFBI to form thicker layers. Just like the WT protein, F-HFBI may assemble through both electrostatic and hydrophobic interactions involving respectively hydrophilic amino acids and the hydrophobic patch. However, for F-HFBI the segregation of the fluorinated domains is also likely to occur due to the scarce affinity of fluorocarbons for both hydrophilic and lipophilic molecules. The presence of an additional self-assembly mechanism may thus lead to thicker protein films.

In order to achieve a deeper structural understanding of the assembly features of F-HFBI films, isothermal compression experiments were carried out at the air–water interface by the Langmuir trough technique. The F-HFBI film was found to have a collapse point of 68.5 mN m^{-1} and a mean molecular area at zero pressure of 96 \AA^2 (Fig. 3b). When compared to the data available in literature for the parent protein NCysHFBI (collapse point of 20 mN m^{-1} and a mean molecular area of 220 \AA^2) [32] and other linear FC-surfactants (collapse points of between 40 and 60 mN m^{-1} and mean molecular areas of around 30 \AA^2) [41,42] the behavior of F-HFBI appears to be more similar to FC-surfactants than to the HFB proteins. This result may indicate that the FC chains are preferentially exposed at the air–water interface, consistent with the very high hydrophobicity of FC segments. The particularly low value of the apparent mean molecular area is not compatible with a protein monolayer, when considering that the typical dimensions of WT-HFBI as derived from its single crystal X-ray structure are about 2–3 nm [43] and therefore supports the hypothesis of the formation of F-HFBI multilayers.

3.4. Adsorption on solid surfaces

The enhanced affinity of F-HFBI for fluoros phases and its tendency to form thicker layers were confirmed also on solid surfaces by Quartz Crystal Microbalance-Dissipation (QCM-D) experiments.

We compared the adsorption behavior of F-HFBI and WT-HFBI on gold surfaces coated with Self-Assembled Monolayers (SAM) of thiols exposing fluorophilic (1H,1H,2H,2H-perfluorodecane-1-thiol), hydrophilic (11-mercapto-1-undecanol), and lipophilic (hexanethiol) alkyl chains. The mass of surface-bound material was determined as well as the viscoelastic properties of the adsorbed layer. Of course, it should be noted that the measured data include contributions from water molecules bound to the protein film. A first estimate of the adsorbed mass can be obtained from observation of the sensor frequency variations displayed by the sensorgrams in Fig. 4, while quantitative data are reported in Table 1.

Both HFBI and F-HFBI bound well to both lipophilic and fluorophilic surfaces. Binding to the hydrophilic surface, instead, was poor in both cases with only small amount of the proteins bound (85 and 137 ng cm^{-2} for HFBI and F-HFBI, respectively). HFBI was found to bind to both lipophilic and fluorophilic surfaces as about a monolayer, in accordance with previous literature data [44] whereas the data obtained for F-HFBI is more consistent with a multilayer assembly and thus a tendency to form thicker protein layers than HFBI. Close examination of the sensorgrams recorded

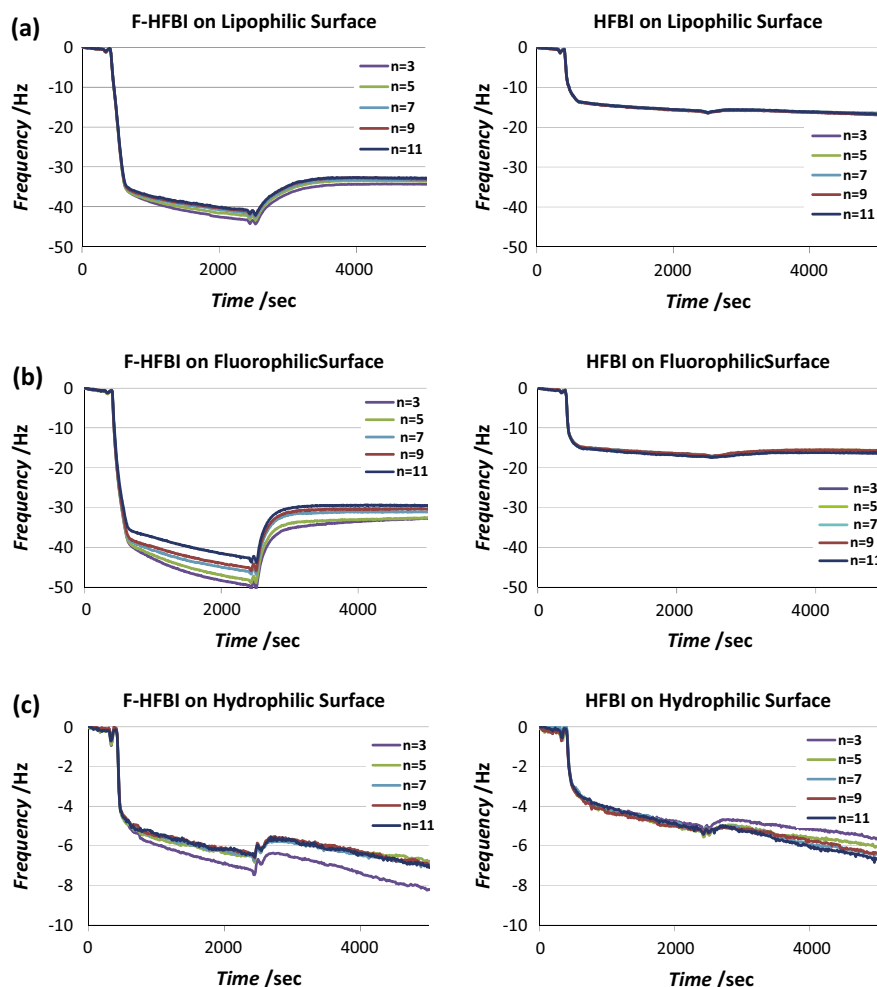


Fig. 4. QCM-D Sensorgrams for F-HFBI (left) and HFBI (right) on various substrates. Data for overtones 3,5,7,9 and 11 are given. (a) lipophilic surface (hexanethiol); (b) fluorophilic surface (1H,1H,2H,2H-perfluorodecane-1-thiol); (c) hydrophilic surface (11-mercapto-1-undecanol). Injection of the protein samples was performed at about 400 s, while rinsing with running buffer was initiated after around 2500 s.

Table 1

Adsorbed amounts of wild-type HFBI and F-HFBI bound to various surfaces determined by QCM-D experiments.

Protein	Surface	Mass adsorbed after washing (ng cm^{-2})
HFBI	Lipophilic	274
F-HFBI	Lipophilic	618
HFBI	Fluorophilic	284
F-HFBI	Fluorophilic	583
HFBI	Hydrophilic	85
F-HFBI	Hydrophilic	137

for each protein on all surfaces also revealed a splitting of the frequency overtones upon F-HFBI binding which was not observed for the wild type protein, accompanied by a simultaneous increase of the recorded dissipation values (for example 2.2 for F-HFBI compared to nearly 0 for HFBI on the fluorophilic surface, as reported in Fig. 5; corresponding data for the other surfaces can be found in Fig. S5 in the Supporting information). This behavior clearly indicates that the protein layer obtained with F-HFBI has a less elastic and more viscoelastic behavior, suggesting that the fluorinated protein forms a less compact and ordered film. The

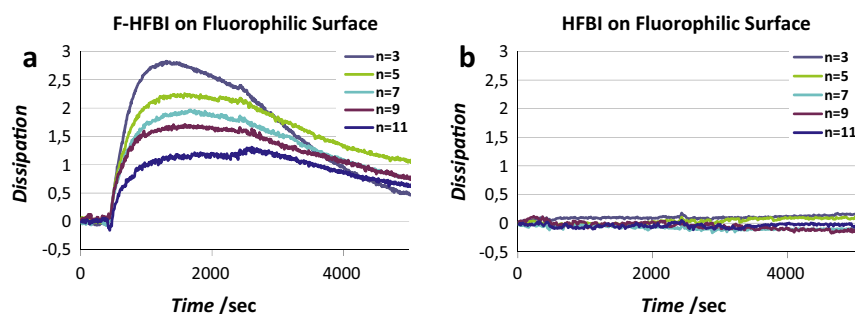


Fig. 5. QCM-D Sensorgrams showing dissipation data for (a) F-HFBI and (b) HFBI on the fluorophilic surface. Overtones 3,5,7,9, and 11 are shown. Protein injection was performed at about 400 s, while rinsing with running buffer was initiated after around 2500 s.

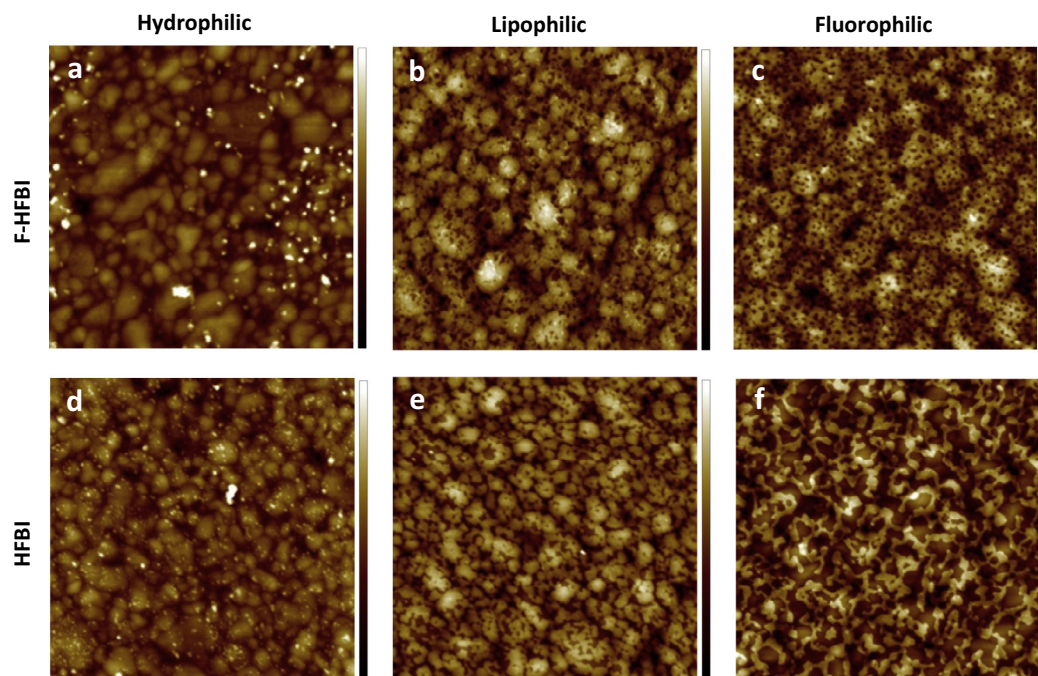


Fig. 6. AFM Images of QCM chips with F-HFBI and HFBI bound to (a and d) a hydrophilic surface, (b and e) a lipophilic surface, and (c and f) a fluorophilic surface. All images represent an area of $1 \times 1 \mu\text{m}$ with a represented height scale of 15 nm.

formation of thicker but less elastic films by F-HFBI in comparison to HFBI is consistent with data obtained previously from interfacial shear rheology and isothermal compression experiments, thus these features at least appear to be common for films formed by adsorption at liquid–liquid and liquid–gas interfaces, on one hand, and on solid surfaces on the other.

The QCM chips coated with HFBI or F-HFBI were dried and analyzed by Atomic Force Microscopy (AFM) and representative images are shown in Fig. 6 (see Fig. S6 in the Supporting information for a representative image of the native gold QCM chip).

Consistent with the data obtained by QCM-D, very small amounts of either protein are seen bound to the hydrophilic surface (Fig. 6a and d), appearing as scattered deposits on top of the bare thiol SAM. Comparison of HFBI and F-HFBI bound to the lipophilic surface (Fig. 6b and e) revealed little difference between the two proteins, as a good coverage is observed in both cases, although small holes can be seen in the films. This is consistent with comparable coating abilities of the two proteins for this substrate.

The greatest difference between the two proteins is observed on the fluorophilic surface, where F-HFBI clearly appears to lead to a better coverage. Examination of images of HFBI on this substrate revealed a discontinuous protein film (Fig. 6f), apparently at variance with the QCM-D results, which suggested coverage of about one monolayer. This apparent inconsistency is supposed to arise from a drying effect where shrinking and breaking of the film occurs as an effect of the strain induced by the receding three-phase line upon water evaporation, thus leading to small patchy areas of protein arranged in multilayers. The hypothesis is supported by the observation that the HFBI deposits on the fluorophilic surface are about 4–5 nm in height from the underlying SAM, whereas a layer thickness of 2.5–3 nm is observed for the same protein adsorbed on the lipophilic substrate. Such behavior suggests that in the case of HFBI adsorption on a fluorophilic SAM, protein–protein interactions are favored with respect to protein–fluorous surface ones, resulting in protein self-aggregation rather than interaction with the substrate, in order to minimize the surface energy. F-HFBI, on the other hand, appears to cover

the surface much better (Fig. 6c), although shrinking upon drying probably still occurs in some measure leading to tiny holes in the protein film. F-HFBI therefore shows an enhanced affinity for the fluorophilic surface, which likely results from the onset of fluorophilic segregation effects involving both the fluorinated thiol of the SAM and the FC moiety of the modified protein, which are expected to be particularly favored in an aqueous environment.

4. Conclusions

In conclusion, we have reported the preparation and characterization of a unique fluorophilic modified hydrophobin, F-HFBI. The reported results show that the modified protein possesses enhanced surface activity with respect to the wild-type HFBI, due to the addition of a fluorocarbon chain. The covalent fluorination did not significantly alter the exceptional self-assembly and film forming features of hydrophobins, while increasing the thickness of films formed. The enhanced fluorophilicity of F-HFBI and its superior capability of coating fluorinated surfaces, as demonstrated by QCM and AFM experiments, make it a particularly appealing compatibilizer for biphasic systems comprising a fluorophilic phase, e.g., (nano)composites involving a fluoropolymer matrix. Research along this direction, as well as the replacement of the perfluoroalkyl chain with a more sustainable perfluoropolyether chain is currently undergoing in our laboratories and will be reported elsewhere.

Acknowledgments

The authors gratefully acknowledge the Academy of Finland for funding (BioHal project, funding decision 260565, P.M., L.P.; SelfSmart project, funding decision 276537, R.M.). The authors also wish to warmly thank Riitta Suihkonen (VTT) for technical support and purification of NCysHFBI as well as for analytical HPLC of F-HFBI. Géza R. Szilvay (VTT) is gratefully acknowledged for the fruitful discussions on protein purification.

Appendix A. Supplementary material

Supplementary data associated with this article can be found, in the online version, at <http://dx.doi.org/10.1016/j.jcis.2015.02.003>.

References

- [1] M.B. Linder, *Curr. Opin. Colloid Interface Sci.* 14 (2009) 356–363, <http://dx.doi.org/10.1016/j.cocis.2009.04.001>.
- [2] M.B. Linder, G.R. Szilvay, T. Nakari-Setälä, M.E. Penttilä, *FEMS Microbiol. Rev.* 29 (2005) 877–896, <http://dx.doi.org/10.1016/j.femsre.2005.01.004>.
- [3] S. Askolin, M.B. Linder, K. Scholtmeijer, M. Tenkanen, M. Penttilä, M.L. de Vocht, H.A.B. Wösten, *Biomacromolecules* 7 (2006) 1295–1301, <http://dx.doi.org/10.1021/bm050676s>.
- [4] T. Subkowski, M. Karos, T. Subkowski, *J. Biotechnol.* 131S (2007) S212–S213, <http://dx.doi.org/10.1016/j.jbiotec.2007.07.382>.
- [5] A. Walther, A.H.E. Muller, *Soft Matter* 4 (2008) 663–668, <http://dx.doi.org/10.1039/B718131K>.
- [6] A.H.Y. Kwan, R.D. Winefield, M. Sunde, J.M. Matthews, R.G. Haverkamp, M.D. Templeton, J.P. Mackay, *Proc. Natl. Acad. Sci. USA* 103 (2006) 3621–3626, <http://dx.doi.org/10.1073/pnas.0505704103>.
- [7] A.R. Cox, F. Cagnol, A.B. Russell, M.J. Izzard, *Langmuir* 23 (2007) 7995–8002, <http://dx.doi.org/10.1021/la700451g>.
- [8] J.A. Gladysz, D.P. Curran, I.T. Horváth, *Handbook of Fluorous Chemistry*, Wiley-VCH, Weinheim, Germany, 2004.
- [9] J.A. Gladysz, D.P. Curran, *Tetrahedron* 58 (2002) 3823–3825, [http://dx.doi.org/10.1016/S0040-4020\(02\)00222-3](http://dx.doi.org/10.1016/S0040-4020(02)00222-3).
- [10] J.-M. Vincent, *J. Fluorine Chem.* 129 (2008) 903–909, <http://dx.doi.org/10.1016/j.jfluchem.2008.06.012>.
- [11] R. Milani, E. Monogioudi, M. Baldrighi, G. Cavallo, V. Arima, L. Marra, A. Zizzari, R. Rinaldi, M.B. Linder, G. Resnati, P. Metrangolo, *Soft Matter* 9 (2013) 6505–6514, <http://dx.doi.org/10.1039/C3SM51262B>.
- [12] M.P. Krafft, J.G. Riess, *Chem. Rev.* 109 (2009) 1714–1792, <http://dx.doi.org/10.1021/cr800260k>.
- [13] A. Zaggia, L. Conte, G. Padoan, R. Bertani, J. Surfact. Deterg. 13 (2010) 33–40, <http://dx.doi.org/10.1007/s11743-009-1136-4>.
- [14] E. Blanco, A. Gonzales-Perez, J.M. Ruso, R. Pedrido, G. Prieto, F. Sarmiento, *J. Colloid Interface Sci.* 288 (2005) 247–260, <http://dx.doi.org/10.1016/j.jcis.2005.02.085>.
- [15] P. Mukerjee, *Physicochem. Eng. Aspects* 84 (1994), [http://dx.doi.org/10.1016/0927-7757\(93\)02682-5](http://dx.doi.org/10.1016/0927-7757(93)02682-5).
- [16] B.E. Smart, *Characteristics of C-F Systems*, in: R.E. Banks, B.E. Smart, J.C. Tatlow (Eds.), *Organofluorine Chemistry: Principles and Commercial Applications*, Plenum Press, New York, USA, 1994.
- [17] M.P. Krafft, *Applications of fluorinated compounds in materials chemistry*, in: J.A. Gladysz, D.P. Curran, I.T. Horváth (Eds.), *Handbook of Fluorous Chemistry*, Wiley-VCH, Weinheim, Germany, 2004.
- [18] C.J. Wilson, D.A. Wilson, A.E. Feiring, V. Percec, *J. Polym. Sci. Part A: Polym. Chem.* 48 (2010) 2498–2508. and references therein <http://dx.doi.org/10.1002/pola.24046>.
- [19] M. Linder, P. Metrangolo, R. Milani, G. Resnati, *Fluorinated hydrophobin and uses thereof* (Fondazione Istituto Italiano di Tecnologia, Valtion Teknillinen Tutkimuskeskus) WO2013080133, 2013.
- [20] B.C. Buer, R. de la Salud-Bea, H.M. Al Hashimi, E.N.G. Marsh, *Biochemistry* 48 (2009) 10810–10817, <http://dx.doi.org/10.1021/bi901481k>.
- [21] E.N.G. Marsh, *Chem. Biol.* 7 (2000) R153–R157, [http://dx.doi.org/10.1016/S1074-5521\(00\)00139-3](http://dx.doi.org/10.1016/S1074-5521(00)00139-3).
- [22] O.-H. Kwon, T.H. Yoo, C.M. Othon, J.A. Van Deventer, D.A. Tirrell, A.H. Zewail, *Proc. Natl. Acad. Sci. USA* 107 (2010) 17101–17106, <http://dx.doi.org/10.1073/pnas.1011569107>.
- [23] B. Holzberger, M. Rubini, H.M. Muller, A. Marx, *Angew. Chem. Int. Ed.* 49 (2010) 1324–1327, <http://dx.doi.org/10.1002/anie.200905978>.
- [24] L. Merkel, N. Budisa, *Org. Biomol. Chem.* 10 (2012) 7241–7261, <http://dx.doi.org/10.1039/C2OB06922A>.
- [25] N. Budisa, W. Wengera, B. Wilttschi, *Mol. BioSyst.* 6 (2010) 1630–1639, <http://dx.doi.org/10.1039/C002256J>.
- [26] C. Jäckel, B. Korsch, *Eur. J. Org. Chem.* (2005) 4483–4503, <http://dx.doi.org/10.1002/ejoc.200500205>.
- [27] M. Cametti, B. Crousse, P. Metrangolo, R. Milani, G. Resnati, *Chem. Soc. Rev.* 41 (2012) 31–42, <http://dx.doi.org/10.1039/C1CS15084G>.
- [28] B.Y.M. Collet, T. Nagashima, M.S. Yu, N.L. Pohl, *J. Fluorine Chem.* 130 (2009) 1042–1048, <http://dx.doi.org/10.1016/j.jfluchem.2009.09.005>.
- [29] E.P. Go, W. Uritboonthai, J.V. Apon, S.A. Trauger, A. Nordstrom, G. O'Maille, S.M. Brittain, E.C. Peters, G. Siuzdak, *J. Proteome Res.* 6 (2007) 1492–1499, <http://dx.doi.org/10.1021/pr060608s>.
- [30] S.M. Brittain, S.B. Ficararo, A. Brock, E.C. Peters, *Nat. Biotech.* 23 (2005) 463–468, <http://dx.doi.org/10.1038/nbt1076>.
- [31] R.K. Kobos, J.W. Eveleigh, R. Arentzen, *Trends Biotech.* 7 (1989) 101–105, [http://dx.doi.org/10.1016/0167-7799\(89\)90008-5](http://dx.doi.org/10.1016/0167-7799(89)90008-5).
- [32] G.R. Szilvay, K. Kisko, R. Serimaa, M.B. Linder, *FEBS Lett.* 581 (2007) 2721–2726, <http://dx.doi.org/10.1016/j.febslet.2007.05.024>.
- [33] F. Höök, M. Rodahl, B. Kasemo, P. Brzezinski, *Proc. Natl. Acad. Sci. USA* 95 (1998) 12271–12276, <http://dx.doi.org/10.1073/pnas.95.21.12271>.
- [34] M.V. Voinova, M. Rodahl, M. Jonson, B. Kasemo, *Phys. Scr.* 59 (1999) 391–396, <http://dx.doi.org/10.1238/Physica.Regular.059a00391>.
- [35] G.R. Szilvay, T. Nakari-Setälä, M.B. Linder, *Biochemistry* 45 (2006) 8590–8598, <http://dx.doi.org/10.1021/bi060620y>.
- [36] S.A. Roberts, I.W. Kellaway, K.M.G. Taylor, B. Warburton, K. Peters, *Int. J. Pharm.* 300 (2005) 48–55, <http://dx.doi.org/10.1016/j.ijpharm.2005.05.003>.
- [37] J.M. Rodriguez Patino, A.L. Caro, M.R. Rodriguez Nino, A.R. Mackie, A.P. Gunning, V.J. Morris, *Food Chem.* 102 (2007) 532–541, <http://dx.doi.org/10.1016/j.foodchem.2006.06.010>.
- [38] S.G. Baldursdottir, M.S. Fullerton, S. Hougaard Nielsen, L. Jorgensen, *Colloids Surf. B* 79 (2010) 41–46, <http://dx.doi.org/10.1016/j.colsurfb.2010.03.020>.
- [39] J.-M. Jung, D.Z. Gunes, R. Mezzenga, *Langmuir* 26 (2010) 15366–15375, <http://dx.doi.org/10.1021/la102721m>.
- [40] A.R. Mackie, A.P. Gunning, M.J. Ridout, P.J. Wilde, V.J. Morris, *Langmuir* 17 (2001) 6593–6598, <http://dx.doi.org/10.1021/la010687g>.
- [41] R. Elbert, T. Folda, H. Ringsdorf, *J. Am. Chem. Soc.* 106 (1984) 7687–7692, <http://dx.doi.org/10.1021/ja00337a005>.
- [42] O. Shibata, M.P. Krafft, *Langmuir* 16 (2000) 10281–10286, <http://dx.doi.org/10.1021/la000929x>.
- [43] J. Hakanpää, G.R. Szilvay, H. Kaljunen, M. Maksimainen, M.B. Linder, J. Rouvinen, *Protein Sci.* 15 (2006) 2129–2140, <http://dx.doi.org/10.1110/pou.062326706>.
- [44] M.S. Grunér, G.R. Szilvay, M. Berglin, M. Lienemann, P. Laaksonen, M.B. Linder, *Langmuir* 28 (2012) 4293–4300, <http://dx.doi.org/10.1021/la300501u>.